

# Bundle Sheath Diffusive Resistance to CO<sub>2</sub> and Effectiveness of C<sub>4</sub> Photosynthesis and Refixation of Photorespired CO<sub>2</sub> in a C<sub>4</sub> Cycle Mutant and Wild-Type *Amaranthus edulis*<sup>1</sup>

Olavi Kiirats, Peter J. Lea, Vincent R. Franceschi, and Gerald E. Edwards\*

School of Biological Sciences, Washington State University, Pullman, Washington 99164–4236 (O.K., V.R.F., G.E.E.); and Department of Biological Sciences, Lancaster University, Lancaster LA1 4YQ, United Kingdom (P.J.L.)

A mutant of the NAD-malic enzyme-type C<sub>4</sub> plant, *Amaranthus edulis*, which lacks phosphoenolpyruvate carboxylase (PEPC) in the mesophyll cells was studied. Analysis of CO<sub>2</sub> response curves of photosynthesis of the mutant, which has normal Kranz anatomy but lacks a functional C<sub>4</sub> cycle, provided a direct means of determining the liquid phase-diffusive resistance of atmospheric CO<sub>2</sub> to sites of ribulose 1,5-bisphosphate carboxylation inside bundle sheath (BS) chloroplasts ( $r_{bs}$ ) within intact plants. Comparisons were made with excised shoots of wild-type plants fed 3,3-dichloro-2-(dihydroxyphosphinoyl-methyl)-propenoate, an inhibitor of PEPC. Values of  $r_{bs}$  in *A. edulis* were 70 to 180 m<sup>2</sup> s<sup>-1</sup> mol<sup>-1</sup>, increasing as the leaf matured. This is about 70-fold higher than the liquid phase resistance for diffusion of CO<sub>2</sub> to Rubisco in mesophyll cells of C<sub>3</sub> plants. The values of  $r_{bs}$  in *A. edulis* are sufficient for C<sub>4</sub> photosynthesis to elevate CO<sub>2</sub> in BS cells and to minimize photorespiration. The calculated CO<sub>2</sub> concentration in BS cells, which is dependent on input of  $r_{bs}$ , was about 2,000 μbar under maximum rates of CO<sub>2</sub> fixation, which is about six times the ambient level of CO<sub>2</sub>. High re-assimilation of photorespired CO<sub>2</sub> was demonstrated in both mutant and wild-type plants at limiting CO<sub>2</sub> concentrations, which can be explained by high  $r_{bs}$ . Increasing O<sub>2</sub> from near zero up to ambient levels under low CO<sub>2</sub>, resulted in an increase in the gross rate of O<sub>2</sub> evolution measured by chlorophyll fluorescence analysis in the PEPC mutant; this increase was simulated from a Rubisco kinetic model, which indicates effective re-fixation of photorespired CO<sub>2</sub> in BS cells.

In C<sub>4</sub> plants, atmospheric CO<sub>2</sub> is fixed via phosphoenolpyruvate carboxylase (PEPC) in mesophyll cells into C<sub>4</sub> acids, which are transported to bundle sheath (BS) cells where they serve as donors of CO<sub>2</sub> to the C<sub>3</sub> cycle via C<sub>4</sub> acid decarboxylases (Kanai and Edwards, 1999). Photosynthetic carbon metabolism in C<sub>4</sub> plants requires low rates of CO<sub>2</sub> leakage from BS cells for CO<sub>2</sub> to be concentrated around Rubisco in the BS chloroplasts. This favors CO<sub>2</sub> fixation and minimizes photorespiration. However, the BS is not impermeable to gases because there is a need for metabolites to be exchanged between it and the mesophyll cells and for O<sub>2</sub> generated during photosynthesis to be released. This permeability causes CO<sub>2</sub> leakage from BS cells and results in a lower energetic efficiency of the CO<sub>2</sub>-concentrating mechanism.

Diffusive resistance of CO<sub>2</sub> into BS cells ( $r_{bs}$ ) has been estimated by measuring photosynthetic rates under varying CO<sub>2</sub> concentrations in isolated BS cells (Furbank et al., 1989) and in excised leaves fed a chemical inhibitor of the C<sub>4</sub> cycle (Jenkins et al.,

1989a; Brown and Byrd, 1993; Brown, 1997), or by applying models to experimental data related to the magnitude of photorespiration in C<sub>4</sub> plants (He and Edwards, 1996). However, accurate determination of  $r_{bs}$  is difficult; current estimates vary over a wide range from about 15 to 1,400 m<sup>2</sup> s<sup>-1</sup> mol<sup>-1</sup> (for review, see He and Edwards, 1996).

BS-diffusive resistance is considered the major component that determines the CO<sub>2</sub> leakage driven by the CO<sub>2</sub> concentration gradient between BS and mesophyll cells. The rate of leakage of CO<sub>2</sub> from the BS cells is equal to the rate of over-cycling of the C<sub>4</sub> pathway (rate of C<sub>4</sub> cycle minus rate of CO<sub>2</sub> fixation by the C<sub>3</sub> cycle). There is considerable variation in estimates of the fraction of CO<sub>2</sub> leakage with various methods, ranging from 0.08 up to 0.5 when expressed as a fraction of C<sub>4</sub> cycle activity (see He and Edwards, 1996). CO<sub>2</sub> leakiness was determined for a number of species using an isotope discrimination method (Henderson et al., 1992) and a method involving analysis of <sup>14</sup>CO<sub>2</sub> release after its fixation (Hatch et al., 1995), with leakiness values ranging from 0.08 to 0.3.

The CO<sub>2</sub> concentration in BS cells is dependent on  $r_{bs}$ , the rate of C<sub>4</sub> pathway over-cycling, and the CO<sub>2</sub> diffusion gradient from BS to mesophyll cells. For a better understanding of C<sub>4</sub> photosynthesis, it would also be valuable to know the actual CO<sub>2</sub> concentration in BS chloroplasts, where CO<sub>2</sub> assimilation takes

<sup>1</sup> This research was supported by the National Science Foundation (grant nos. IBN-9807916 and IBN-0131098 to G.E.E.).

\* Corresponding author; e-mail edwardsg@wsu.edu; fax 509-335-3184.

Article, publication date, and citation information can be found at [www.plantphysiol.org/cgi/doi/10.1104/pp.008201](http://www.plantphysiol.org/cgi/doi/10.1104/pp.008201).

place. A possible means of estimating this is to combine measurements of CO<sub>2</sub> fixation with information on the kinetic properties of Rubisco. Ribulose 1,5-bisphosphate (RuBP) carboxylation and oxygenation in BS chloroplasts are competing reactions, and information is available on the Rubisco CO<sub>2</sub> to O<sub>2</sub> affinity ratio.

In this study, we have used the PEPC mutant of *Amaranthus edulis* LaC<sub>4</sub> 2.16 (Dever et al., 1995; Maroco et al., 1998a, 1998b), which has a defective C<sub>4</sub> cycle and requires direct diffusion of atmospheric CO<sub>2</sub> into the BS cells for CO<sub>2</sub> assimilation and growth. In this mutant, the primary carboxylase for fixing atmospheric CO<sub>2</sub> is Rubisco, which is located in the BS chloroplast. The purpose of this work was to use gas exchange measurements on the *A. edulis* mutant for direct estimation of BS cell resistance to CO<sub>2</sub>, and to determine the dependence of  $r_{bs}$  on the developmental stage of the leaf. For comparison, data were also obtained with wild-type plants by feeding the PEPC inhibitor 3,3-dichloro-2-(dihydroxyphosphinoyl-methyl)-propenoate (DCDP) to prevent operation of the C<sub>4</sub> cycle. In addition, we determined rates of CO<sub>2</sub> fixation and gross rates of O<sub>2</sub> evolution to analyze the effect of temperature on the cellular conductance to CO<sub>2</sub> and the effects of CO<sub>2</sub>, light, and O<sub>2</sub> on partitioning of electron flow and refixation of photorespired CO<sub>2</sub>.

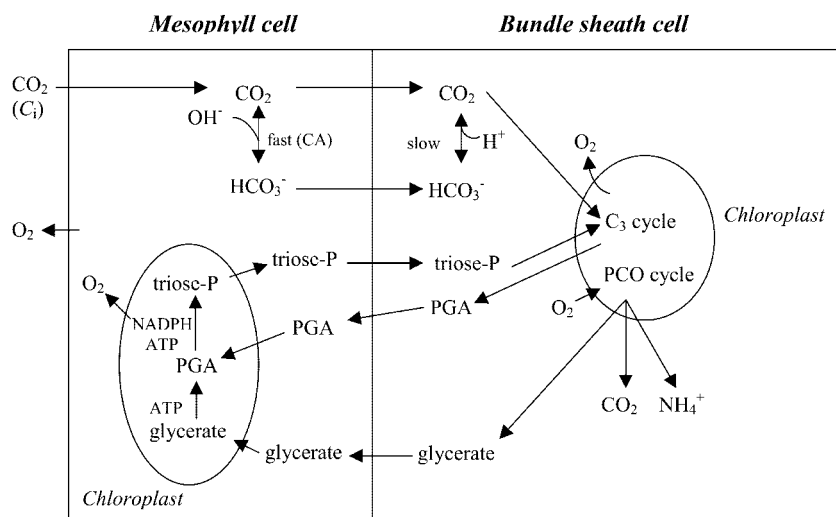
## RESULTS AND DISCUSSION

Figure 1 outlines important aspects of photosynthesis in the PEPC mutant of *A. edulis* relative to the experimental approach for determining the BS-diffusive resistance to CO<sub>2</sub> ( $r_{bs}$ ). Because the C<sub>4</sub> cycle is inoperative, the mechanism of CO<sub>2</sub> fixation and energy requirements are considered the same as in C<sub>3</sub> plants. Fixation of atmospheric CO<sub>2</sub> in the mutant by Rubisco in the C<sub>3</sub> cycle, requires diffusion of CO<sub>2</sub> from the mesophyll to BS cells. CO<sub>2</sub> is considered the

primary species of inorganic carbon diffusing to BS cells and supplying CO<sub>2</sub> to Rubisco. Although CO<sub>2</sub> will be converted rapidly to bicarbonate in the cytosol of mesophyll cells via carbonic anhydrase, the diffusion pathway for bicarbonate will be limited because it is not used by Rubisco and BS cells lack, or have negligible levels of, carbonic anhydrase (Ku and Edwards, 1975). Also, in wild-type *A. edulis*, where CO<sub>2</sub> is concentrated in the BS cells by the C<sub>4</sub> cycle through C<sub>4</sub> acid decarboxylation, CO<sub>2</sub> is considered the primary form of inorganic carbon leaking from BS to mesophyll cells (Jenkins et al., 1989b). Reaction of O<sub>2</sub> with RuBP in the photosynthetic carbon oxidation cycle in the BS chloroplasts will result in the production of the photorespiratory products glycerate, CO<sub>2</sub>, and ammonia through metabolism in mitochondria and peroxisomes. According to the known compartmentalization of carbon assimilation in C<sub>4</sub> plants (Kanai and Edwards, 1999), the only function of mesophyll chloroplasts in carbon assimilation in the mutant may be the conversion of glycerate, the product of photorespiration in BS cells, to triose phosphate and conversion of some of the 3-phosphoglycerate (PGA), generated by Rubisco in BS cells, to triose phosphate.

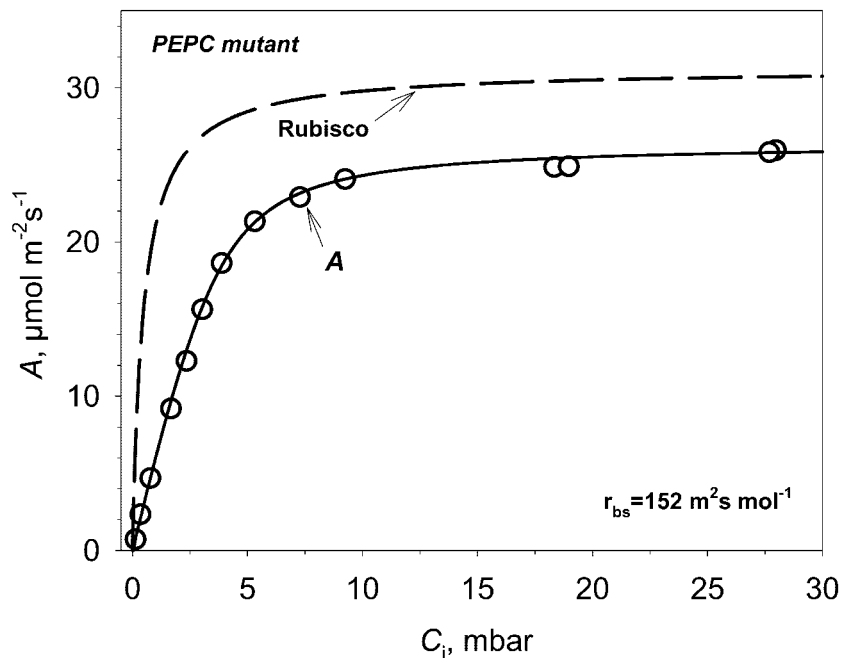
### BS-Diffusive Resistance to CO<sub>2</sub> ( $r_{bs}$ )

The resistances involved in uptake of atmospheric CO<sub>2</sub> by the mutant are described in Equation 10 ("Materials and Methods"). If the CO<sub>2</sub> response curve of CO<sub>2</sub> assimilation (measured at light saturation) is plotted against the intercellular CO<sub>2</sub> partial pressure ( $C_i$ ), which equilibrates with the liquid phase at the cell wall, the initial slope of the curve is determined by the average physical liquid phase conductance and by the carboxylation efficiency of Rubisco (Fig. 2). Gas phase resistance to CO<sub>2</sub>,  $r_s$ , was calculated based on transpiration measurements. Typical values of  $r_s$  for the mutant plants were in the



**Figure 1.** Schematic representation of the movement of gases and metabolites in the PEPC mutant of *A. edulis*. CO<sub>2</sub> diffuses into BS cell chloroplasts where it enters the C<sub>3</sub> cycle. Equilibrium between HCO<sub>3</sub><sup>-</sup> and CO<sub>2</sub> in mesophyll cell is fast, but it is slow in BS because of lack of carbonic anhydrase activity. Glycerate, ammonia, and CO<sub>2</sub> are generated by the photosynthetic carbon oxidation (PCO) cycle. Glycerate metabolism and partial reduction of PGA in mesophyll cells may account for use of some photochemically generated energy in mesophyll chloroplasts.

**Figure 2.** Example of calculating BS cell resistance from  $A$  versus  $C_i$  curves measured at low  $O_2$  (0.3 mbar) and PFD of  $1,800 \mu\text{mol m}^{-2} \text{s}^{-1}$  in PEPC mutant. The inverse of the initial slope of  $A/C_i$  curve is the sum of the diffusive resistance from the cell wall to the sites of Rubisco and of the chemical RuBP carboxylation resistance. A simulated Rubisco  $\text{CO}_2$  response curve without diffusive resistance is shown for comparison. Rubisco resistance can be calculated as  $K_c/V_c$ .  $V_c$  was taken as  $A_{\text{max}}$ .



range of  $5$  to  $10 \text{ m}^2 \text{ s}^{-1} \text{ mol}^{-1}$  ( $2$ – $4 \text{ s cm}^{-1}$ ). Also, the expected Rubisco  $\text{CO}_2$  response curve is shown in Figure 2 in the absence of liquid phase resistance; this demonstrates the contribution of the resistance of RuBP carboxylase (chemical resistance),  $r_c$ , to the total  $\text{CO}_2$  flux resistance. The Rubisco response was generated taking the maximum velocity of RuBP carboxylase ( $V_c$ ) as  $1.2$  times the  $\text{CO}_2$ -saturated rate of  $\text{CO}_2$  fixation ( $A_{\text{max}}$ ) based on Rubisco extractable activity measurements. Also, there is a decrease in RuBP pool with increasing  $\text{CO}_2$ , which could account for  $A_{\text{max}}$  being lower than  $V_c$  of Rubisco if RuBP becomes limiting (as shown later in Fig. 7). In general,  $r_c$  for mutant leaves was a minor component (from  $10$  to  $15 \text{ m}^2 \text{ s}^{-1} \text{ mol}^{-1}$ ) compared with  $r_{\text{bs}}$  ( $152 \text{ m}^2 \text{ s}^{-1} \text{ mol}^{-1}$  in Fig. 2).

Analogous experiments to those in Figure 2 were performed on leaves of different maturity. The value of  $r_{\text{bs}}$  increased with plant age and reached its highest value during grain filling when the leaves were pale

green, showing early signs of senescence and lower maximum rates of  $\text{CO}_2$  fixation (Table I). Although BS resistance was calculated assuming  $V_c$  is  $1.2$  times  $A_{\text{max}}$ , a sensitivity analysis taking  $V_c/A_{\text{max}} = 1.0$  and  $1.4$  showed that this results in a change in the calculated  $r_{\text{bs}}$  values of only  $3\%$  to  $5\%$  in young leaves, and approximately  $2\%$  in mature leaves. Interestingly, during the grain filling stage, the leaves still maintained a reasonably high- $\text{CO}_2$  assimilation capacity. The liquid phase resistance from the mesophyll cells to Rubisco in the mutant *A. edulis* ( $72$ – $181 \text{ m}^2 \text{ s}^{-1} \text{ mol}^{-1}$ ; Table I) is about  $70$ -fold higher than that of  $C_3$  plants (approximately  $1$ – $3 \text{ m}^2 \text{ s}^{-1} \text{ mol}^{-1}$ ; Evans et al., 1994; Laisk and Loreto, 1996). This high-diffusive resistance in  $C_4$  plants may be attributed to the relatively low BS cell surface area per unit leaf area and structural properties of BS cell walls (Evans and von Caemmerer, 1996). Models of  $C_4$  photosynthesis indicate the rate of  $\text{CO}_2$  assimilation under low  $\text{CO}_2$  drops rapidly below  $r_{\text{bs}}$  values of  $50$  to  $100 \text{ m}^2 \text{ s}^{-1} \text{ mol}^{-1}$

**Table I.** Leaf age-dependent differences in  $A_{\text{max}}$  and resistance to  $\text{CO}_2$  in the *A. edulis* PEPC mutant plants

The mesophyll to BS resistance for  $\text{CO}_2$  was calculated as the inverse of the initial slope of  $A/C_i$  curves. The SD for mesophyll to BS resistance and  $A_{\text{max}}$  was calculated from four independent measurements.  $r_{\text{bs}}$  was calculated according to the method used in Figure 2.  $A_{\text{max}}$  was the  $\text{CO}_2$ -saturated rate of photosynthesis, and other conditions of the assay were as in Figure 2.

Leaf Description	$A_{\text{max}}$	Mesophyll to BS	Liquid Phase
		Resistance to $\text{CO}_2$ ( $r_{\text{bs}} + r_c$ )	Resistance to $\text{CO}_2$ ( $r_{\text{bs}}$ )
	$\mu\text{mol m}^{-2} \text{ s}^{-1}$	$\text{m}^2 \text{ s}^{-1} \text{ mol}^{-1}$	
Young, 30% expanded	$25.1 \pm 1.4$	$89 \pm 16$	$72.4$
Young, 70% expanded	$26.6 \pm 1.8$	$103 \pm 16$	$86.3$
Mature, vegetative, 100% expanded	$30.6 \pm 1.0$	$127 \pm 6$	$113.4$
Grain filling stage, 100% expanded	$20.6 \pm 1.2$	$201 \pm 17$	$180.8$

(Edwards et al., 2000; Laisk and Edwards, 2000; von Caemmerer, 2000).

The resistance observed in the mutant might not reflect the true value of the wild type if the mutation alters the structure of the BS cells. To test this, we used the PEPC inhibitor DCDP, feeding it into the petiole to block the C<sub>4</sub> cycle in wild-type plants (method of Jenkins et al., 1989a). The strong reduction in carboxylation efficiency caused by 4 mM DCDP, without a biphasic response (Fig. 3), suggests that PEPC is almost completely inhibited. CO<sub>2</sub> response curves were measured at 2% (v/v) O<sub>2</sub> before applying DCDP and immediately after photosynthesis declined at ambient CO<sub>2</sub> as PEPC was inhibited (Fig. 3). The results show that the calculated BS resistances are similar to those obtained with the PEPC mutant. We measured A/C<sub>i</sub> response curves (C<sub>i</sub> determined from analysis of transpiration, which eliminates stomatal resistance) and calculated the resistance from the initial slope with V<sub>c</sub> for Rubisco equal to 1.2 A<sub>max</sub> estimated from CO<sub>2</sub>-saturated rates in the presence of DCDP. In calculating r<sub>bs</sub>, it is important to eliminate stomatal resistance and to account for any partial inhibition of Rubisco, and V<sub>c</sub>, by DCDP. Jenkins et al. (1989a) calculated a permeability coefficient for CO<sub>2</sub> from the atmosphere to BS cells (the reciprocal for the total diffusive resistance, r<sub>t</sub>) from

measurements of photosynthetic O<sub>2</sub> evolution in the presence of DCDP at 1.6% (v/v) CO<sub>2</sub> by dividing the photosynthetic rate by the difference between atmospheric CO<sub>2</sub> (C<sub>a</sub>) and estimates of C<sub>BS</sub>. The calculated value of r<sub>t</sub> from the study of Jenkins et al. in *A. edulis* is 556 s · cm<sup>-1</sup> (or 1,373 m<sup>2</sup> s<sup>-1</sup> mol<sup>-1</sup>), which is about 10-fold higher than values of r<sub>bs</sub> in the present study. Because r<sub>t</sub> includes stomatal and BS-diffusive resistance, high stomatal resistance in excised leaves could contribute to high r<sub>t</sub> values. Our A/C<sub>i</sub> response curves with the PEPC mutant saturate sharply at intercellular CO<sub>2</sub> concentrations about 1%, whereas up to 5% (v/v) ambient CO<sub>2</sub> was required in experiments by Jenkins et al. (1989). Also, the calculation of r<sub>t</sub> is dependent on input of V<sub>c</sub> of Rubisco to calculate C<sub>BS</sub>. Using the value of V<sub>c</sub> from analysis of wild-type plants (Jenkins et al., 1989), rather than V<sub>c</sub> in the presence of DCDP, will also overestimate V<sub>c</sub> and the calculated diffusive resistance values (see also He and Edwards, 1996).

Light microscopy of leaf anatomy indicates that the wild-type plants grown under both 370 μbar and 10 mbar and the PEPC mutant grown under 10 mbar of CO<sub>2</sub> all have Kranz-type leaf anatomy (results not shown; Dever et al., 1995). In wild-type plants grown at 10 mbar of CO<sub>2</sub>, the BS cell walls at the intercellular space are very thick relative to the walls of the

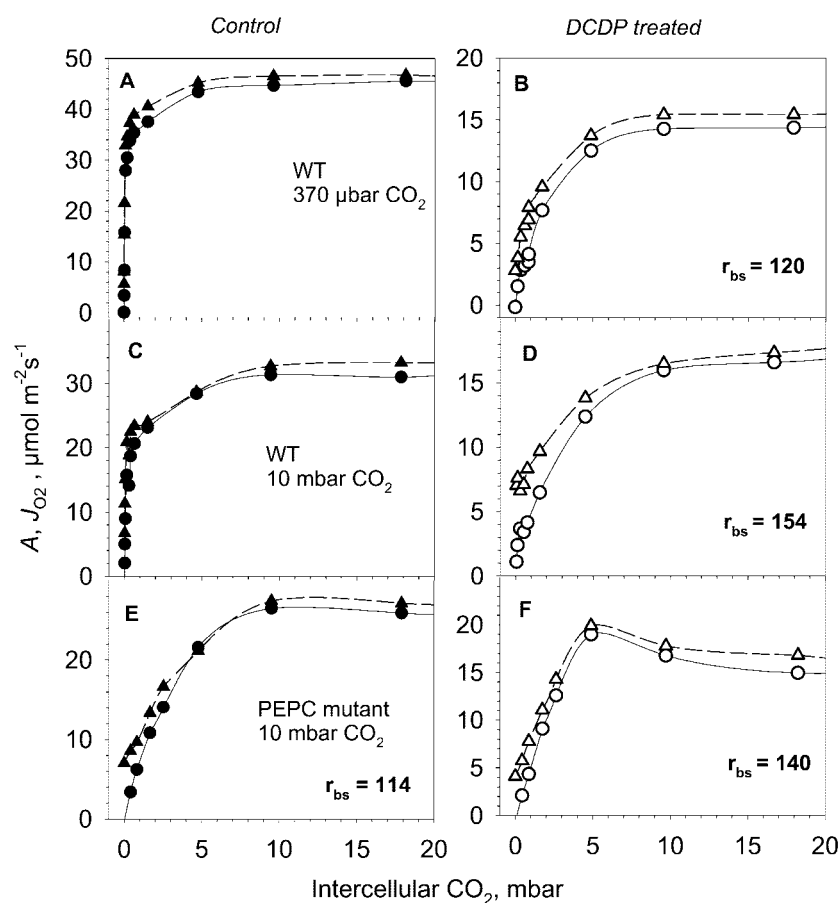


**Figure 3.** The response of the rates of CO<sub>2</sub> assimilation (A, ○, ●) and gross rate of O<sub>2</sub> evolution from PSII (J<sub>O<sub>2</sub></sub>, ▲, △) on wild type and PEPC mutant with and without feeding DCDP. Measurements were made on leaves of excised plants under 20 mbar O<sub>2</sub>. The calculated values of r<sub>bs</sub> in wild-type plants in presence of DCDP and in PEPC mutant with and without DCDP are shown. A and B, Wild-type plants grown at 370 μbar CO<sub>2</sub>; C and D, wild-type plants grown at 10 mbar CO<sub>2</sub>; E and F, PEPC mutant grown at 10 mbar CO<sub>2</sub>.

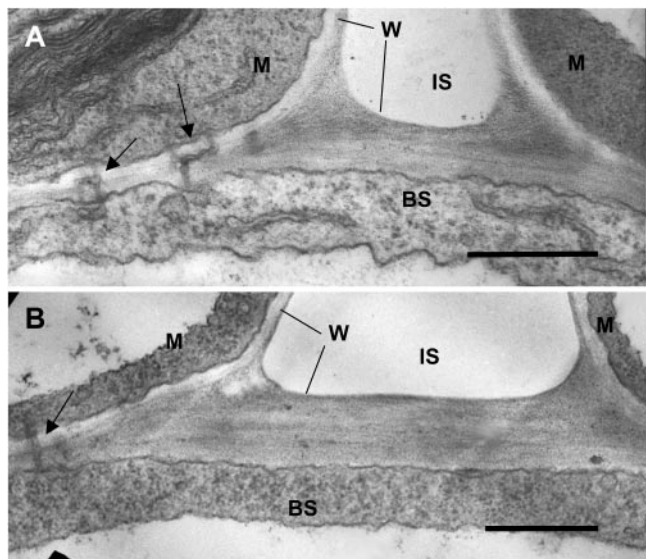


**Figure 4.** Electron microscopy showing cross sections through interface of mesophyll and BS of leaves of wild type (A) and PEPC mutant (B) with plants grown at 10 mbar CO<sub>2</sub>. M, Part of mesophyll cell; BS, part of BS cell; W, cell wall; IS, intercellular air space. Arrows point to plasmodesmata. Scale bar = 0.5 μm. The average thickness of BS cell wall in contact with intercellular air from several sections was 0.34 μm for wild type and 0.32 μm for mutant (n = 3).

mesophyll and cross walls (Fig. 4); similar results were obtained with wild type grown under ambient CO<sub>2</sub>. In the PEPC mutant, the BS cell walls are also much thicker than those of mesophyll cells, and cross walls include normal plasmodesmata (arrow). This suggests there are no structural differences between mutant and wild type.

**Cellular Conductance and the Temperature Dependence of Photosynthesis under Limiting and Saturating CO<sub>2</sub>**

CO<sub>2</sub> response curves of photosynthesis were measured in wild-type and mutant *A. edulis* at leaf temperatures from 15°C to 35°C. Figure 5, A and B, describes the temperature response of  $A_{max}$ , determined from CO<sub>2</sub>-saturated rates, and cellular conductance for CO<sub>2</sub>,  $g$ , determined from the initial slope of the net rate of CO<sub>2</sub> assimilation ( $A/C_i$ ) curves. In this case, conductance instead of resistance ( $g = 1/r$ ) was used, because it is linearly related to the diffusion flux. In wild-type plants, the cellular conductance for CO<sub>2</sub>,  $g_{wt}$  was a function of liquid phase diffusion and carboxylation by PEPC in the mesophyll cell. For the mutant,  $g_{mut}$  was the total conductance from mesophyll to BS cells, including liquid phase ( $g_{bs}$ ) and Rubisco ( $g_c$ ), as determined earlier.

$A_{max}$  increased with increasing temperature, with a  $Q_{10}$  value (the factor by which a reaction increases with a 10°C increase in temperature) of 2 for the mutant and 1.9 for the wild type between 20°C and 30°C. The corresponding activation energies were  $E_a = 13.5$  and  $11.3 \text{ kcal mol}^{-1}$  (Fig. 5C, calculated

between 20°C and 30°C). These values of  $Q_{10}$  and activation energies are as expected if photosynthesis under saturating CO<sub>2</sub> and light is controlled by enzymatic processes. Also, the activation energy for  $A_{max}$  in the mutant ( $13.5 \text{ kcal mol}^{-1}$ ) was close to the in vitro Rubisco activation energy of  $13 \text{ kcal mol}^{-1}$  (calculated from Jordan and Ogren, 1984). If RuBP is

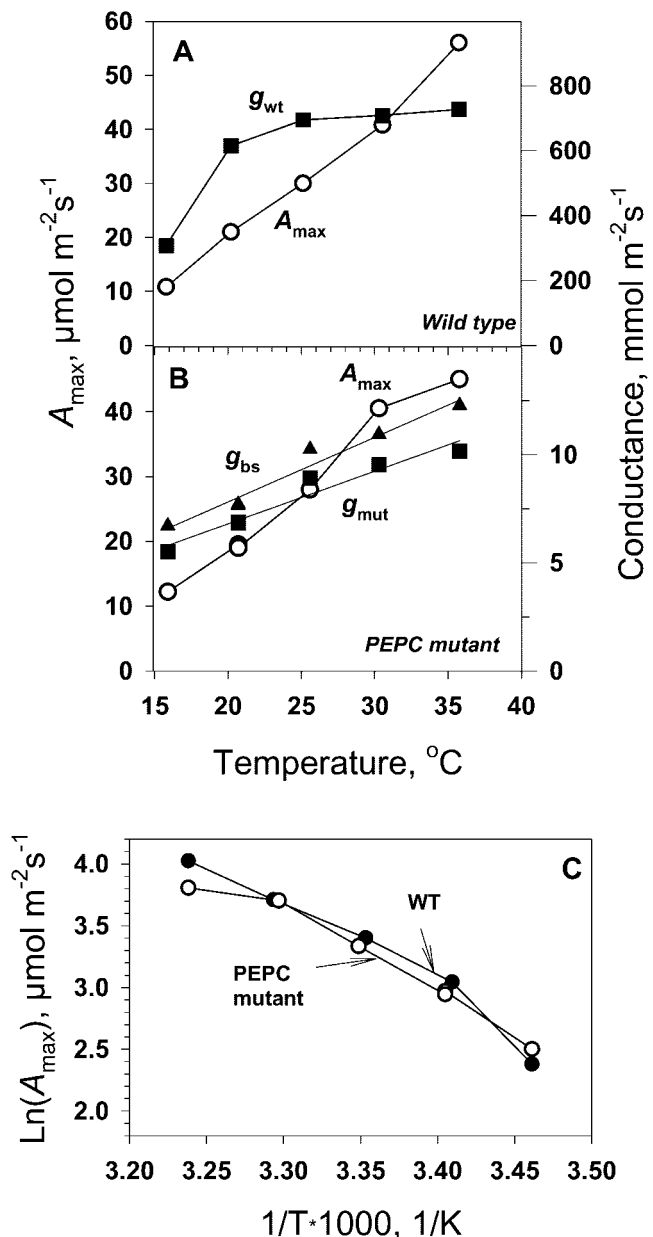


**Figure 5.** Temperature dependence of photosynthetic parameters for wild-type (A) and PEPC mutant (B) *A. edulis* measured under 0.3 mbar O<sub>2</sub>. Shown are internal conductance in the mesophyll for wild type,  $g_{wt}$  (the initial slope of  $A/C_i$  curves), the internal conductance in the mutant,  $g_{mut}$ , and the calculated liquid phase-diffusive conductance in the mutant ( $g_{bs}$ ) and maximal CO<sub>2</sub> assimilation rate ( $A_{max}$ ). C has  $A_{max}$  from A and B plotted in Arrhenius axes (the slope equals  $-E_a/R$ ). Values of  $J_{O_2-net}$  measured under saturating CO<sub>2</sub> (data not shown) were similar to values of  $A_{max}$ .

saturation for photosynthesis under high light, the  $Q_{10}$  values obtained would be consistent with Rubisco, rather than a diffusion limitation, being the major limiting factor for light- and CO<sub>2</sub>-saturated photosynthesis in the mutant.

In the mutant,  $g_{mut}$  (which includes  $g_{bs}$  and Rubisco conductance) and  $g_{bs}$  had a linear response to increasing temperature. For  $g_{bs}$ , the  $Q_{10}$  values were 1.3 between 20°C and 30°C (Fig. 5B), which coincides with the temperature sensitivity of diffusion of small molecules in solutions that have a  $Q_{10}$  value of 1.3 (Nobel, 1991). The agreement between the measured and expected  $Q_{10}$  value for  $g_{bs}$  provides confidence that we are correctly measuring diffusive resistance of CO<sub>2</sub> to BS cells. Because CO<sub>2</sub> must diffuse to BS cells for fixation in the mutant, the cellular conductance values for the mutant are much lower than for the wild type.

In wild-type plants, CO<sub>2</sub> is fixed initially in mesophyll cells, and the temperature response of the mesophyll conductance, determined from the initial slope of the CO<sub>2</sub> response curve, showed a saturating curve rather than a linear response, indicating that biochemistry is involved (Fig. 5A). The effect of temperature on the initial slope of the  $A/C_i$  response in wild-type *A. edulis* depends on liquid phase diffusion and PEPC in mesophyll cells. The relative insensitivity of the mesophyll conductance in the wild type to temperature indicates control by biochemistry. This could be attributable to regulation of PEPC by temperature-dependent changes in  $K_m$  for phosphoenolpyruvate (PEP; the substrate PEP is lower under limiting CO<sub>2</sub> [Leegood and von Caemmerer, 1988]), by allosteric effectors, and/or by covalent modification of the enzyme (phosphorylation/dephosphorylation). There also may be a temperature-dependent effect on PEP because the level is reported to increase with increasing temperature under normal atmospheric levels of CO<sub>2</sub> (Labate et al., 1990).

### CO<sub>2</sub> Response and Partitioning of Photochemical Electron Flow

The CO<sub>2</sub> response curves for CO<sub>2</sub> fixation ( $A$ ), gross rates of O<sub>2</sub> evolution ( $J_{O_2}$ ), and net rates of O<sub>2</sub> evolution ( $J_{O_2-net}$ ) of the mutant and wild-type leaves were measured at saturating light (Fig. 6). Measurements of  $A$  and  $J_{O_2}$  were made at 210 mbar of O<sub>2</sub>, representing current atmospheric levels, and measurements of  $A$ ,  $J_{O_2}$ , and  $J_{O_2-net}$  at near zero levels of O<sub>2</sub> (0.3 mbar), with an interest in studying O<sub>2</sub>-dependent processes. To overcome the high-diffusive resistance from the atmosphere to the BS cells in the mutant, CO<sub>2</sub> concentrations as high as 2% (20 mbar) were required (Fig. 6, A and C), whereas near atmospheric levels were saturating for the wild type (Fig. 6, B and D). The mutant plants of *A. edulis* had about 100 times lower initial slopes in  $A/C_i$  curves compared with the wild type (Fig. 6, A versus B and C

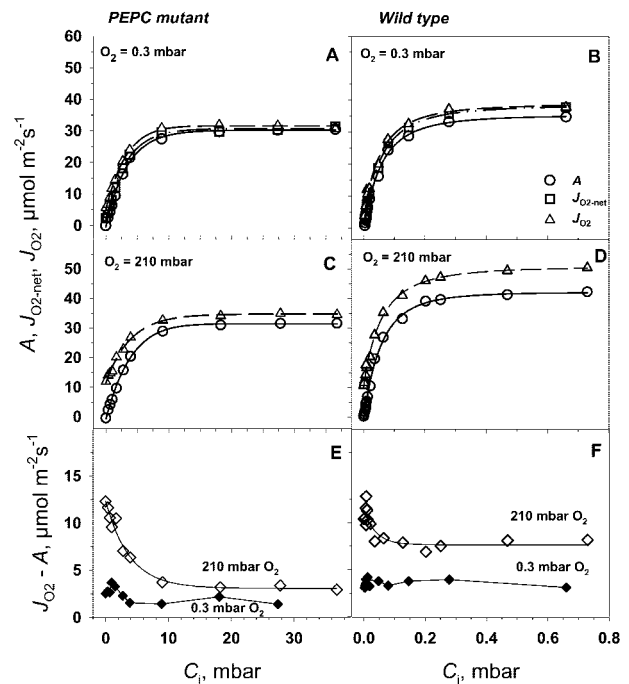


**Figure 6.** The response of the rates of CO<sub>2</sub> assimilation ( $A$ , ○), net O<sub>2</sub> evolution ( $J_{O_2-net}$ , □), and gross O<sub>2</sub> evolution from PSII ( $J_{O_2}$ , △) in PEPC mutant and wild-type *A. edulis* to intercellular CO<sub>2</sub> ( $C_i$ ) at two oxygen partial pressures, 210 and 0.3 mbar. The CO<sub>2</sub> response curves were measured at PFD = 1,800 μmol m<sup>-2</sup> s<sup>-1</sup> and at leaf temperature 29°C.

versus D). From various measurements of  $A_{max}$  at 30°C during the course of the study on young to mature leaves, values were usually 30 to 40 μmol m<sup>-2</sup> s<sup>-1</sup> in the mutant compared with 40 to 50 μmol m<sup>-2</sup> s<sup>-1</sup> in the wild type. It is apparent that rates of  $A$ ,  $J_{O_2}$ , and  $J_{O_2-net}$  were very similar in both the mutant and wild type at 0.3 mbar O<sub>2</sub> (Fig. 6, A and B). At 210 mbar of O<sub>2</sub>,  $J_{O_2}$  was substantially higher than  $A$  in both mutant and wild type (Fig. 6, C and D). This is clearly shown in Figure 6, E and F, where  $J_{O_2}-A$  is plotted in response to varying CO<sub>2</sub> at 0.3 and 210 mbar of O<sub>2</sub>.  $J_{O_2}-A$  can potentially be accounted for by dark-type mitochondrial respiration ( $R_d$ ), photorepiration (1.5 velocity of RuBP oxygenase [ $v_o$ ]), photosystem (PS) II-dependent O<sub>2</sub> evolution associated with the Mehler-peroxidase reaction ( $J_{O_2MR}$ ), and O<sub>2</sub> evolution associated with nitrogen assimilation ( $J_{O_2NA}$ ; see Eqs. 3–6).

In the mutant at 0.3 mbar of O<sub>2</sub>, it is obvious that most of the PSII activity ( $J_{O_2}$ ) can be accounted for by CO<sub>2</sub> fixation and that  $R_d$ ,  $v_o$ ,  $J_{O_2MR}$ , and  $J_{O_2NA}$  must be low (Fig. 6, A and E). Because a partial pressure of 0.3 mbar of O<sub>2</sub> in the atmosphere is extremely low, a correspondingly low level is expected in the mesophyll cells within the leaf. However, even under very low external levels of O<sub>2</sub>, the O<sub>2</sub> level in the BS cells will increase when O<sub>2</sub> is generated from PSII activity under a high-BS cell-diffusive resistance. At 0.3 mbar of O<sub>2</sub> in the atmosphere and based on the average

value for BS cell resistance determined in this study (described later), the calculated level of O<sub>2</sub> in BS cells at CO<sub>2</sub>-saturated rates of photosynthesis was about 30 mbar. From Equation 14, if we take  $A = 30 \mu\text{mol m}^{-2} \text{s}^{-1}$ ,  $r_{\text{bs}} = 30 \text{ s cm}^{-1}$  ( $80 \text{ m}^2 \text{ s}^{-1} \text{ mol}^{-1}$ ),  $a_w = 0.79$  ( $a_w$  is a constant that takes into account the difference in O<sub>2</sub> and CO<sub>2</sub> diffusivities [at 25°C,  $a_w = 0.79$ ; Farquhar, 1983]), and  $b = 0.5$ , then the concentration of O<sub>2</sub> would be 35 μM (equivalent to about 30 mbar of O<sub>2</sub> in the gas phase;  $O_2 = 0 + 0.79 \cdot 0.5 \cdot 30 \cdot A / 10 = 35 \mu\text{M}$ ).  $R_d$  from measurements in the dark under normal atmospheric conditions is 2 to 3 μmol m<sup>-2</sup> s<sup>-1</sup> (data not shown). On average,  $J_{O_2NA}$  for nitrate assimilation to Glu is estimated to be about 5% of  $A$ , not considering re-assimilation of ammonia from photorespiration (see Edwards and Baker, 1993). Thus,  $R_d$  in vascular tissue plus nitrate assimilation could easily account for the difference between  $J_{O_2}$  and  $A$  at 0.3 mbar of O<sub>2</sub>. Some rise in values of  $J_{O_2-A}$  under limiting CO<sub>2</sub> at 0.3 mbar of O<sub>2</sub> would be expected, because  $A$  decreases relative to  $R_d$  (Fig. 6E). These results indicate that  $J_{O_2Mr}$  and  $v_o$  must be very low in the mutant under 0.3 mbar of O<sub>2</sub> in the atmosphere.

In the mutant at 210 mbar of O<sub>2</sub>, the values of  $J_{O_2-A}$  were much greater than at 0.3 mbar of O<sub>2</sub>, particularly with decreasing levels of CO<sub>2</sub> (Fig. 6E). The logical explanation for this effect is that the mutant, which lacks a C<sub>4</sub> cycle, has increasing rates of photorespiration under limiting CO<sub>2</sub> just as C<sub>3</sub> plants do (see also Lacuesta et al., 1997; Maroco et al., 1998a), which causes a corresponding increase in  $J_{O_2}$ . Under high CO<sub>2</sub> and under 210 mbar of O<sub>2</sub>, the mutant may have some additional dark-type respiration in mesophyll cells, resulting in larger values of  $J_{O_2-A}$  than at 0.3 mbar of O<sub>2</sub>.

In the wild-type plant under 0.3 mbar of O<sub>2</sub> (Fig. 6F), the value of  $J_{O_2-A}$  was about 4 μmol m<sup>-2</sup> s<sup>-1</sup>, which was higher than in the mutant, and was independent of the level of CO<sub>2</sub>. As with the mutant, nitrate as-

simulation and  $R_d$  in BS tissue may partly account for the difference. However, the Mehler reaction or photorespiration may also contribute in the wild-type plant. In a recent study, there was evidence for significant Mehler reaction in wild-type *A. edulis* under rather low levels of O<sub>2</sub> (between 0.2 and 20 mbar; Laik and Edwards, 1998). In NAD-malic enzyme (NAD-ME) species like *A. edulis*, the Mehler reaction is proposed to function in mesophyll chloroplasts and contribute to generation of ATP for the C<sub>4</sub> cycle (Furbank and Badger, 1982; Laik and Edwards, 1998). With increasing CO<sub>2</sub>, there may be a rise in the rate of the Mehler reaction as the rate of the C<sub>4</sub> cycle increases, whereas with decreasing CO<sub>2</sub>, there may be a rise in photorespiration; together these effects could result in values of  $J_{O_2-A}$  being reasonably constant in NAD-ME-type species with varying CO<sub>2</sub> (see Furbank and Badger, 1982).

In the wild-type plant under 210 mbar of O<sub>2</sub>,  $J_{O_2}$  was higher than  $A$  across the CO<sub>2</sub> response curve (Fig. 6D); the pattern of change with increasing CO<sub>2</sub> is very similar to that of Canvin et al. (1980) from O<sub>2</sub> isotope analysis of photosynthesis in *A. edulis*.  $J_{O_2-A}$  at 210 mbar was greater than at 0.3 mbar of O<sub>2</sub>, and a sharp increase in  $J_{O_2-A}$  occurred at very low levels of CO<sub>2</sub>. Above approximately 0.025 mbar of CO<sub>2</sub>,  $J_{O_2-A}$  was constant at about 8 μmol m<sup>-2</sup> s<sup>-1</sup> (Fig. 6F). As noted above, this can be explained by O<sub>2</sub>-dependent photorespiration at extremely low levels of CO<sub>2</sub> and increasing Mehler reaction at higher CO<sub>2</sub>. The larger  $J_{O_2-A}$  values at high CO<sub>2</sub> under 210 mbar versus 0.3 mbar of O<sub>2</sub> may be accounted for by O<sub>2</sub>-dependent dark respiration and/or the Mehler reaction.

To evaluate Rubisco kinetics in mutant leaves relative to  $A$  and  $J_{O_2}$ , we analyzed RuBP content and Rubisco activity (Fig. 7). With increasing CO<sub>2</sub> from zero up to about 0.8 mbar there was an increase in RuBP content, above which it decreased. The initial

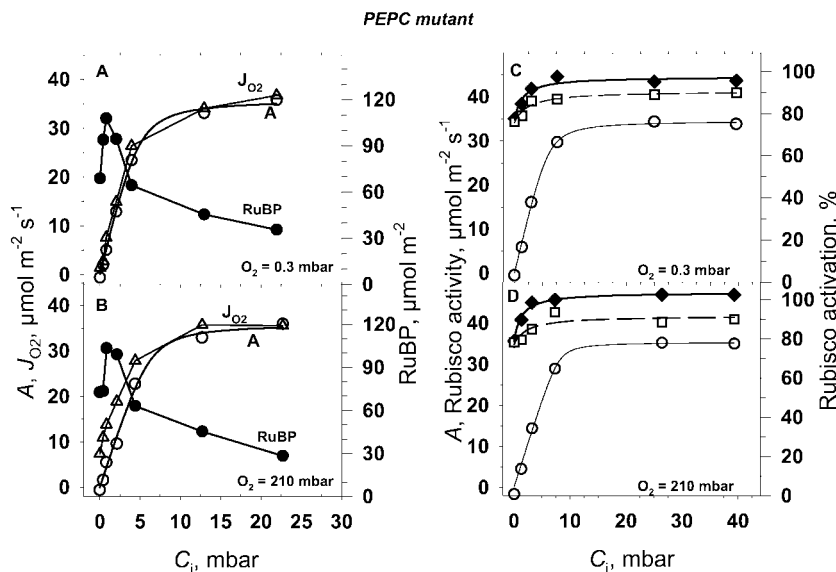


**Figure 7.** CO<sub>2</sub> response for CO<sub>2</sub> assimilation rate (A, O), gross O<sub>2</sub> evolution rate (J<sub>O<sub>2</sub></sub>, Δ), RuBP pool size (●), Rubisco activity (◆), and Rubisco activation state (□) for PEPC mutant *A. edulis* at two O<sub>2</sub> pressures, 0.3 and 210 mbar. Leaf temperature was 28°C, PFD = 1,400 μmol m<sup>-2</sup> s<sup>-1</sup>. Each point is from a different leaf of similar age.

extractable activity of Rubisco in the mutant was higher than  $A_{\max}$  at saturating CO<sub>2</sub> and decreased slightly at the lower CO<sub>2</sub> concentrations (Fig. 7, C and D). The decrease at low CO<sub>2</sub> correlated with a decrease in the state of activation of the enzyme. In the wild type (results not shown), leaf RuBP content was similar to the mutant at low CO<sub>2</sub> (at CO<sub>2</sub> = 34  $\mu$ bar, RuBP was 56  $\mu$ mol m<sup>-2</sup>) and decreased at high CO<sub>2</sub> (at CO<sub>2</sub> = 4.8 mbar, RuBP was 47  $\mu$ mol m<sup>-2</sup>), which is in close agreement with the values of Leegood and von Caemmerer (1988). Considering a Rubisco active site turnover rate of 2.8 s<sup>-1</sup> (Woodrow and Berry, 1988), the number of active sites per leaf area in *A. edulis* would be about 15 to 20  $\mu$ mol m<sup>-2</sup>. The RuBP concentration across the  $A/C_i$  curve at light saturation exceeded the number of active sites by about three times, which suggests the RuBP is at saturating levels. However, the observation that the RuBP concentration decreased at high CO<sub>2</sub> (Fig. 7) and with the known competitive interaction of some chloroplast metabolites with RuBP (e.g. PGA; Servaites and Geiger, 1995), it is possible that  $A_{\max}$  is partly limited by RuBP regeneration.

#### Light Response and Partitioning of Photochemical Electron Flow

The response of photosynthesis to light under very high CO<sub>2</sub> (4%, 40 mbar) in the mutant gave about the same maximal quantum yield for O<sub>2</sub> evolution ( $J_{O_2\text{-net}}/J_{O_2}$ ) as in the wild type (0.064 versus 0.066; Fig. 8, A and B). The quantum yield for O<sub>2</sub> evolution for wild-type *A. edulis* was higher than measured by Ehleringer and Bjorkman (1977) for CO<sub>2</sub> fixation in NAD-ME-type C<sub>4</sub> species (0.054). Higher values for the wild type may be explained by the use of highly saturating CO<sub>2</sub> and very low O<sub>2</sub>, which would restrict O<sub>2</sub>-dependent use of energy, and by the fact that O<sub>2</sub> evolution, rather than CO<sub>2</sub> uptake, was measured. In the wild-type plant under very high CO<sub>2</sub>, the responses of  $J_{O_2}$  and  $J_{O_2\text{-net}}$  to increasing light were very similar, indicating there was little photorespiration and Mehler reaction under this condition. It is uncertain why the Mehler reaction would be restricted under such high levels of CO<sub>2</sub> in the wild type. However, in the wild-type plant under 4% (v/v) CO<sub>2</sub>, direct diffusion of CO<sub>2</sub> to BS cells would occur, bypassing the C<sub>4</sub> cycle, because in mutant plants, which lack a C<sub>4</sub> cycle, photosynthesis is saturated by 2% (v/v) CO<sub>2</sub>.

In the mutant, under saturating levels of CO<sub>2</sub>, which prevent photorespiration, we would expect maximum quantum yields of O<sub>2</sub> evolution similar to those of C<sub>3</sub> plants. Instead, the values in the mutant were lower than in C<sub>3</sub> plants under saturating CO<sub>2</sub> and similar to those of the *A. edulis* wild type. This suggests that the absorbed energy, which is used in the wild type in mesophyll chloroplasts for the C<sub>4</sub> cycle (ATP for conversion of pyruvate to PEP, and

NADPH to the degree malate is synthesized), may be dissipated as heat in the mutant if there is no other means for using it in carbon assimilation. In the mutant, there is no requirement for energy in mesophyll cells in carbon assimilation, unless part of the PGA and glycerate formed via RuBP carboxylase and oxygenase activities in BS chloroplasts is shuttled to mesophyll cells for reduction (Fig. 1).

In the mutant under CO<sub>2</sub> which is limiting for photosynthesis (2 mbar), and at 210 mbar of O<sub>2</sub>,  $J_{O_2}$  was much higher than  $A$ , and the maximum quantum yield under limiting light was higher for  $J_{O_2}$  than for  $A$  (Fig. 8C). This can be explained by the mutant having a high level of photorespiration and responding like a C<sub>3</sub>-type species under limiting CO<sub>2</sub>.

In the wild type under atmospheric levels of CO<sub>2</sub> and 210 mbar O<sub>2</sub>, the light response curves showed a higher quantum yield (from initial slopes) and a higher light-saturated rate for  $J_{O_2}$  than for  $A$  (Fig. 8D). This may be attributed to the Mehler reaction increasing with increasing light and generating ATP for the C<sub>4</sub> cycle under 210 mbar O<sub>2</sub>, which could largely account for the difference between  $J_{O_2}$  and  $A$ . With the wild-type plant having a functional C<sub>4</sub> cycle, photorespiration and dark-type respiration are expected to be minor components of the difference between  $J_{O_2}$  and  $A$ . A previous study indicated that the Mehler reaction is functioning in *A. edulis* but is insufficient to supply the ATP needed to support the C<sub>4</sub> cycle (Laisk and Edwards, 1998). Thus, both the Mehler reaction and PSI-mediated cyclic electron flow may generate the ATP, with some flexibility in the magnitude of each. In contrast to results under

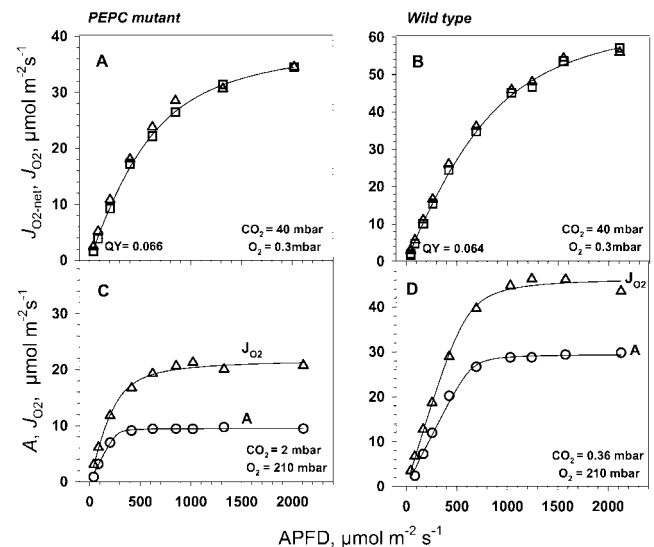


**Figure 8.** Light response of PEPC mutant and wild-type *A. edulis* O<sub>2</sub> evolution ( $J_{O_2\text{-net}}$ ,  $\square$ ) at highly saturating levels of CO<sub>2</sub> of 40 mbar CO<sub>2</sub> (O<sub>2</sub> = 0.3 mbar), and CO<sub>2</sub> uptake ( $A$ ,  $\circ$ ) at limiting CO<sub>2</sub> (2 mbar for PEPC mutant and 0.36 mbar for wild type) and 210 mbar O<sub>2</sub> pressure. Leaf temperature was 28°C. Gross rates of O<sub>2</sub> evolution ( $J_{O_2}$ ,  $\Delta$ ) were calculated from simultaneous fluorescence measurements as described in "Materials and Methods."

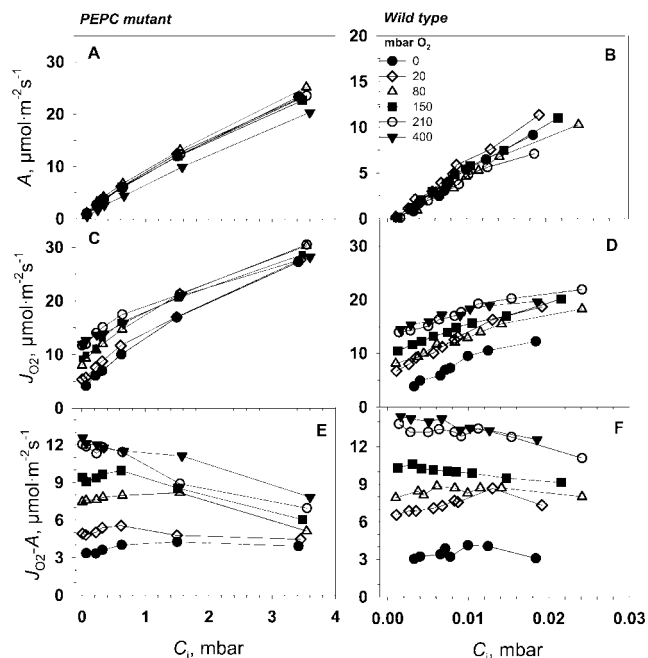


**Figure 9.** Oxygen sensitivity of *A. edulis* photosynthesis at limiting CO<sub>2</sub> concentrations, 30°C, and PFD = 1,800 μmol m<sup>-2</sup> s<sup>-1</sup>. The rate of PSII O<sub>2</sub> evolution ( $J_{O_2}$ ) shows an increase with increasing O<sub>2</sub> concentration and continues at CO<sub>2</sub> = 0 because of re-assimilation of CO<sub>2</sub> released from the photorespiration and from the Krebs cycle.

210 mbar of O<sub>2</sub> (Figs. 6D and 8D), there was no evidence for function of the Mehler reaction under low O<sub>2</sub> (Fig. 8B), which suggests the ATP needed to support the C<sub>4</sub> cycle is provided by PSI-dependent cyclic electron flow.

**O<sub>2</sub> Effect on the Partitioning of Photochemical Electron Flow**

It is well known that at low-CO<sub>2</sub> concentrations, the rate of CO<sub>2</sub> assimilation in C<sub>4</sub> plants exhibits low sensitivity to O<sub>2</sub>. This is in contrast to C<sub>3</sub> plants, where photorespiration greatly reduces the rate of CO<sub>2</sub> assimilation in response to increasing O<sub>2</sub> (Kanai and Edwards, 1999). Measurements of *A* and  $J_{O_2}$  in mutant plants, in which the C<sub>4</sub> cycle is not functional, provide an opportunity to follow more closely the maximum potential for Rubisco oxygenase and the glycolate pathway to function. This is not possible in normal C<sub>4</sub> leaves, where the CO<sub>2</sub> pump operates.

The responses of *A* and  $J_{O_2}$  were measured at increasing O<sub>2</sub> concentrations over a range of CO<sub>2</sub>-limited concentrations where greater RuBP oxygenase activity is expected for mutant and wild-type plants (Fig. 9). In the wild-type plant at rate-limiting CO<sub>2</sub> levels, high O<sub>2</sub> increased  $J_{O_2}$ , but the CO<sub>2</sub> assimilation rates remained relatively unaffected by O<sub>2</sub> (Fig. 9, B and D). The increase in  $J_{O_2}$  with increasing O<sub>2</sub> under low CO<sub>2</sub> suggests an increase in photorespiration through RuBP oxygenase activity. At a given level of O<sub>2</sub>, the value of  $J_{O_2}$ -*A* (Fig. 9F) re-

mained about the same with increasing levels of CO<sub>2</sub>, which, as discussed earlier, may be attributable to the Mehler reaction partially providing ATP to support the C<sub>4</sub> cycle and increasing with increasing rates of CO<sub>2</sub> fixation.

In the mutant, high O<sub>2</sub> increased  $J_{O_2}$  at the lowest, rate-limiting CO<sub>2</sub> levels, but the CO<sub>2</sub> assimilation rates remained relatively unaffected by O<sub>2</sub> (Fig. 9, A and C). The increased electron transport rate with increasing O<sub>2</sub> under limiting CO<sub>2</sub> suggests an O<sub>2</sub>-dependent increase in the RuBP oxygenation rate. At the higher levels of O<sub>2</sub>, the difference between  $J_{O_2}$  and *A* (Fig. 9E) was gradually suppressed by increasing CO<sub>2</sub>, which is expected if increasing CO<sub>2</sub> suppresses photorespiration and considering that the mutant does not have a C<sub>4</sub> cycle that could be supported by the Mehler reaction.

For the mutant under limiting CO<sub>2</sub>, the activity of  $J_{O_2}$  is expected to be largely accounted for by the sum of the velocity of RuBP carboxylase ( $v_c$ ) and  $v_o$ . We extrapolated  $J_{O_2}$ , measured at different O<sub>2</sub> concentrations, to CO<sub>2</sub> = 0 and plotted the resulting values against BS cell O<sub>2</sub> concentration in an effort to evaluate the effect of Rubisco oxygenase activity on  $J_{O_2}$  (Fig. 10). Assuming photorespired CO<sub>2</sub> is re-assimilated with the probability determined by the ratio of Rubisco conductance to BS cell conductance, the expected  $J_{O_2}$  response can be described by the solid line in Figure 10. The experimental points are in good agreement with predicted results based on Rubisco kinetics if re-assimilation is accounted for, except that at the highest O<sub>2</sub> level (480 μM, which is

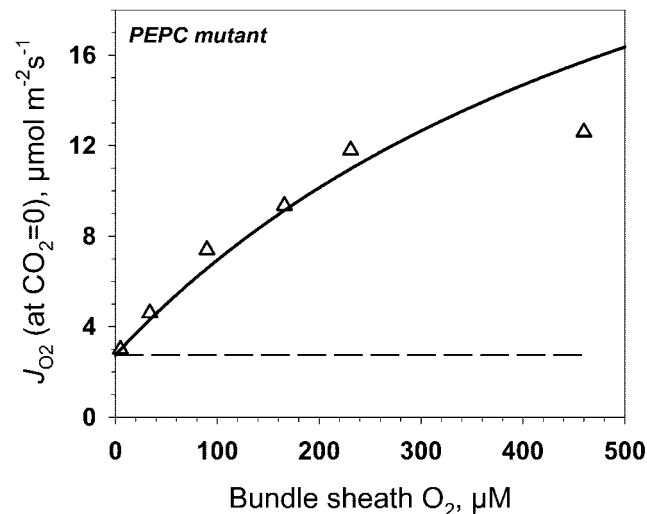


**Figure 10.**  $J_{O_2}$  for the PEPC mutant of *A. edulis* from Figure 9 was extrapolated to CO<sub>2</sub> = 0, and the results were plotted against O<sub>2</sub> concentration. The simulated  $J_{O_2}$  shown by the solid line was calculated based on BS O<sub>2</sub> and CO<sub>2</sub> concentration (the latter calculated for each O<sub>2</sub> level considering BS-diffusive resistance) and Rubisco kinetic constants ( $V_c = 39$ ,  $K_c = 21$  μM, and  $K_o = 640$  μM), where  $J_{O_2}$  equals  $v_c + v_o$  (Edwards and Baker, 1993). The rate of CO<sub>2</sub> re-assimilation (at zero external CO<sub>2</sub>) is proportional to the ratio of Rubisco conductance and BS-diffusive conductance.

about twice the atmospheric level), the oxygenase activity was lower than expected. Analysis of RuBP content in the leaves of the mutant at low CO<sub>2</sub> (0.4 mbar) showed a decrease of RuBP concentration at rate-limiting CO<sub>2</sub> and with increasing O<sub>2</sub> (Fig. 11). Therefore, we suggest that the lower than expected  $J_{O_2}$  value at O<sub>2</sub> concentration below the  $K_m$  for RuBP oxygenase ( $K_o$ ) value (640  $\mu\text{M}$ ) in the mutant (Fig. 10) is the result of RuBP becoming partially limiting for CO<sub>2</sub> assimilation. Very similar results were obtained with wild-type plants (Fig. 11). Also, the response of  $J_{O_2}$  to O<sub>2</sub>, under low CO<sub>2</sub>, in the wild type is similar to that in *A. edulis* measured at the CO<sub>2</sub> compensation point by O<sub>2</sub> isotope analysis (Canvin et al., 1980).

There was only a small effect of O<sub>2</sub> on the rate of CO<sub>2</sub> assimilation at low-CO<sub>2</sub> concentrations in either the mutant or wild-type *A. edulis* (Fig. 9). The limited effect of O<sub>2</sub> on CO<sub>2</sub> assimilation in the mutant, where

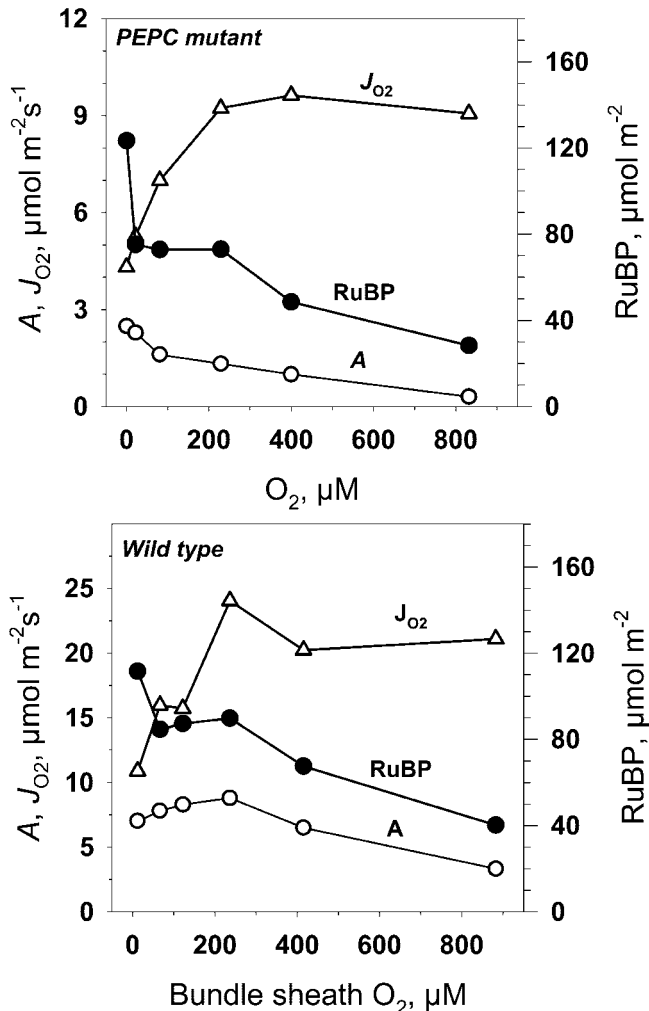


**Figure 11.** PEPC mutant and wild-type *A. edulis* leaf RuBP content (●) versus O<sub>2</sub> concentration with C<sub>i</sub> of 0.4 mbar for mutant and 0.025 mbar for wild type. Also, CO<sub>2</sub> assimilation rate (A, ○) and O<sub>2</sub> evolution from PSII ( $J_{O_2}$ , △) are shown. Leaf temperature was 28°C; light PFD = 1,800  $\mu\text{mol m}^{-2} \text{s}^{-1}$ .

there is no C<sub>4</sub> cycle function, can be explained by effective re-assimilation in the BS cells of the CO<sub>2</sub> that is generated from dark-type respiration and photorespiration. It is also evident that in the wild-type plants, CO<sub>2</sub> re-assimilation at low CO<sub>2</sub> affects assimilation kinetics. In this case, refixation of photorespired CO<sub>2</sub> may occur in mesophyll cells via PEPC, if there is leakage of CO<sub>2</sub>, as well as in BS cells. However, the effectiveness of the mutant suggests that, under low CO<sub>2</sub>, much of the photorespired CO<sub>2</sub> will be directly refixed in BS cells.

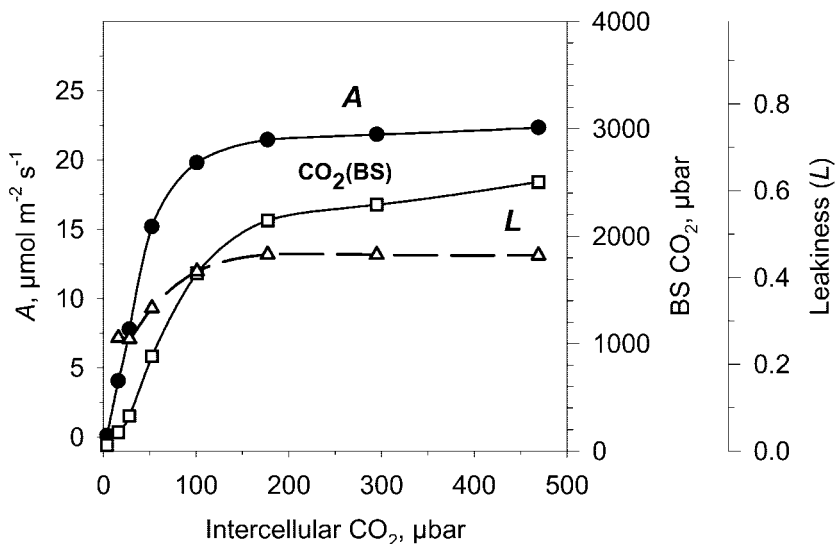
#### Calculation of CO<sub>2</sub> Concentration and Leakiness of CO<sub>2</sub> in BS Cells of *A. edulis*

If Rubisco kinetic parameters ( $V_c$ ,  $K_c$  [the  $K_m$  for RuBP carboxylase],  $K_o$ , and  $S$  [the relative specificity factor for carboxylase versus oxygenase]) are known, one can calculate BS CO<sub>2</sub> concentration using a C<sub>4</sub> photosynthesis model (von Caemmerer, 2000). Figure 12 shows calculated BS cell CO<sub>2</sub> concentrations during photosynthesis in wild-type *A. edulis* leaves under varying intercellular CO<sub>2</sub> concentrations at 210 mbar of O<sub>2</sub> calculated with the model of C<sub>4</sub> photosynthesis. Also, shown in Figure 12 are the calculated values of BS cell leakiness during CO<sub>2</sub> fixation in wild-type plants, which range from approximately 0.2 to 0.3 (from Eqs. 16 and 17, using an  $r_{bs}$  value of 113  $\text{m}^2 \text{s}^{-1} \text{mol}^{-1}$ ). As increasing ambient levels of CO<sub>2</sub> became saturating for photosynthesis, the calculated levels of CO<sub>2</sub> in the BS cells of mature leaves reached levels of approximately 2,000  $\mu\text{bar}$ , which is about six times that normally occurring in the atmosphere.

#### CONCLUDING REMARKS

The PEPC mutant of *A. edulis* has high light- and CO<sub>2</sub>-saturated rates of photosynthesis comparable with those of the wild type. The high CO<sub>2</sub> required for growth and the high-diffusive resistance of the PEPC mutant to CO<sub>2</sub> indicate that physical restraints to gases have been conserved in the C<sub>4</sub> anatomy of the mutant. The value of BS cell resistance to CO<sub>2</sub> increased with leaf age in *A. edulis* from 72 to 181  $\text{m}^2 \text{s}^{-1} \text{mol}^{-1}$  (Table I). Similar resistance values for mature leaves were obtained with wild-type plants treated with the PEPC inhibitor DCDP. The results suggest there may be developmental changes in BS cells that increase the diffusive resistance to CO<sub>2</sub> by changes in the liquid phase of the cell or cell wall properties. The concentration of CO<sub>2</sub> in BS cells under high rates of photosynthesis is estimated to be about six times current ambient levels, sufficient to largely repress photorespiration. Re-assimilation of CO<sub>2</sub> from dark-type respiration and photorespiration in BS cells is an important component of both PSII activity and consumption of reductive power at very low-CO<sub>2</sub> concentrations in *A. edulis*.

**Figure 12.** CO<sub>2</sub> response for CO<sub>2</sub> assimilation rate (at leaf temperature of 28°C; PFD = 1,800 μmol m<sup>-2</sup>s<sup>-1</sup>; ●), calculated CO<sub>2</sub> partial pressure in BS cells (□), and leakiness of CO<sub>2</sub> from BS cells (Δ). The CO<sub>2</sub> level in BS cells was calculated according to von Caemmerer (2000), and the leakiness was calculated according to equations 16 and 17 using *r*<sub>bs</sub> value of 113 m<sup>2</sup> s<sup>-1</sup> mol<sup>-1</sup>. Similar results were obtained from analysis of several experiments on *A/C<sub>i</sub>* responses.



## MATERIALS AND METHODS

### Growth Conditions

Mutant plants of *Amaranthus edulis* LaC<sub>4</sub> 2.16 lacking PEPC activity and protein (Dever et al., 1995) were grown in growth chambers (Econair, Winnipeg, Canada) on fertilized potting soil in 8-L pots (one plant per pot), with a 14/10-h day/night cycle at 28°C/22°C, 50% relative humidity, 10 mbar of CO<sub>2</sub>, and an incident photosynthetically quantum flux density (PFD) of 1,200 μmol m<sup>-2</sup> s<sup>-1</sup> light. Wild-type plants were grown under the same conditions, except the CO<sub>2</sub> concentration was 370 μbar and 10 mbar in experiments with DCDP and electron microscopy and 370 μbar in all other experiments.

### Gas Exchange (*A* and *J*<sub>O<sub>2</sub>-net</sub>)

Leaf gas exchange was measured with the FastEst gas system (FastEst, Tartu, Estonia; described in detail in Laisk and Oja, 1998). The system was equipped with a CO<sub>2</sub> analyzer (6251, LI-COR, Lincoln, NE) and a S-3A O<sub>2</sub> ceramic heated zirconium oxide analyzer (Applied Electrochemistry Inc., Sunnyvale, CA). Leaf gas exchange characteristics, net rates of CO<sub>2</sub> fixation (*A*), *C<sub>i</sub>*, PFD, and leaf temperature were determined as in Laisk and Loreto (1996). For measurements of *A* under high levels of CO<sub>2</sub>, there is an increase in noise to signal ratio in measuring CO<sub>2</sub> with an infrared gas analyzer. To improve measurements of *A*, sampling time was 0.1 s for 3 min resulting in 1,800 data points, which were averaged. For example, in one experiment *A* measured at 3% (v/v) CO<sub>2</sub> was 41.9 μmol m<sup>-2</sup> s<sup>-1</sup> with a SE with *n* = 1,800 of ± 0.12. The S-3A O<sub>2</sub> analyzer provides an accurate measure of the net rate of O<sub>2</sub> evolution (*J*<sub>O<sub>2</sub>-net</sub>) under low levels of atmospheric O<sub>2</sub> (less than 10 mbar), independent of CO<sub>2</sub> concentration.

### Measurement of Chlorophyll Fluorescence and Calculation of PSII Activity (*J*<sub>O<sub>2</sub></sub>)

The yield of PSII was measured by chlorophyll fluorescence using a fluorometer (PAM 101, Walz, Effeltrich, Germany). The gross rate of O<sub>2</sub> evolution from PSII (*J*<sub>O<sub>2</sub></sub>) was calculated as:

$$J_{O_2} = \text{APFD} \cdot Y_{II'} \cdot (F_m' - F_s) / F_m' / 4 \quad (1)$$

where  $(F_m' - F_s) / F_m'$  is the yield of PSII (*e*<sup>-</sup> quanta absorbed), *F<sub>s</sub>* is fluorescence yield of steady-state photosynthesis, *F<sub>m</sub>'* is maximal fluorescence yield by exposure to a 1-s pulse of 15,000 μmol m<sup>-2</sup> s<sup>-1</sup> light and APFD is the absorbed photosynthetic quantum flux density at steady state (Genty et al., 1989). For estimating the relative optical cross section of PS II (*Y<sub>II'</sub>*), the method proposed by Laisk and Loreto (1996) was used. *Y<sub>II'</sub>* was found by extrapolating a plot of *F<sub>s</sub>*/*F<sub>m</sub>'* versus quantum yield of O<sub>2</sub> evolution mea-

sured with an O<sub>2</sub> electrode (*J*<sub>O<sub>2</sub>-net</sub>) at different light intensities, to *F<sub>s</sub>*/*F<sub>m</sub>'* = 0. The measurements were made under a low-O<sub>2</sub> background (0.025%) and high CO<sub>2</sub> so that respiratory uptake of O<sub>2</sub> would be minimized and the O<sub>2</sub> evolution measured would reflect essentially all PSII activity. The calculated values of *Y<sub>II'</sub>* for wild-type and mutant plants were 0.44 to 0.55 and 0.41 to 0.48, respectively. For calculations of APFD, the light reflected and transmitted by the leaf was measured using an integrating sphere (Labsphere, North Sutton, NH). For the mutant leaf, the average fractional absorption of incident light was 0.82, whereas for the wild type, the value was 0.85. In mature leaves of mutant plants, the chlorophyll (a+b) content was 156 mg m<sup>-2</sup> compared with 309 mg m<sup>-2</sup> in the ambient CO<sub>2</sub>-grown wild type. The fresh weights of the mutant and wild-type leaves were identical, 22 mg cm<sup>-2</sup>, but the mutant had less dry weight per leaf area, 2.9 mg cm<sup>-2</sup>, compared with 4.4 mg cm<sup>-2</sup> in the wild type (leaves were sampled at midday).

### Equations and Calculation of Leaf Photosynthesis Parameters

#### O<sub>2</sub> Evolution in Mutant and Wild Type

O<sub>2</sub> evolution associated with linear electron transport rate can be expressed as

$$J_{O_2} = v_c + v_o + J_1 \quad (2)$$

where *v<sub>c</sub>* and *v<sub>o</sub>* are RuBP carboxylation and oxygenation rates, respectively, and *J<sub>1</sub>* is the use of electrons in other processes (e.g. Mehler reaction and nitrogen reduction). The following equations illustrate the main factors in considering the relationship between *J*<sub>O<sub>2</sub></sub>, *J*<sub>O<sub>2</sub>-net</sub>, and *A* in C<sub>3</sub> and C<sub>4</sub> plants, because there is no net consumption of reductive power in the C<sub>4</sub> cycle of malic enzyme-type species (see Edwards and Baker, 1993).

$$A = v_c - 0.5v_o - R_d \quad (3)$$

$$J_{O_2} = v_c + v_o + J_{O_{2Mf}} + J_{O_{2NA}} \quad (4)$$

$$J_{O_2} = A + R_d + 1.5v_o + J_{O_{2Mf}} + J_{O_{2NA}} \quad (5)$$

$$J_{O_2\text{-net}} = A + J_{O_{2NA}} \quad (6)$$

where *R<sub>d</sub>* = rate of dark-type mitochondrial respiration, *J*<sub>O<sub>2Mf</sub></sub> = PSII-dependent O<sub>2</sub> evolution associated with the Mehler-peroxidase reaction, and *J*<sub>O<sub>2NA</sub></sub> = O<sub>2</sub> evolution associated with nitrogen assimilation (reduction of nitrate and assimilation to Glu).

### Analysis of Parameters of CO<sub>2</sub> Fixation and $r_{bs}$ in PEPC Mutant

We assume that light-saturated CO<sub>2</sub> uptake in the mutant *A. edulis* plants is limited primarily by physical diffusive resistance to CO<sub>2</sub> and Rubisco activity (see Fig. 1). Values for the diffusive resistance to CO<sub>2</sub>, carboxylation resistance, and RuBP carboxylation and oxygenation velocities can be calculated from leaf gas exchange measurements using the biochemical model of Rubisco developed by Farquhar et al. (1980). According to their model for C<sub>3</sub> photosynthesis, the CO<sub>2</sub> assimilation rate in the mutant can be described according to equation 3 above, where  $A = v_c - 0.5 v_o - R_d$ . Assuming Rubisco saturation by RuBP,

$$v_c = \frac{V_c \cdot C_c}{C_c + K_c(1 + O_c/K_o)} \quad (7)$$

$$v_o = \frac{V_o \cdot O_c}{O_c + K_o(1 + C_c/K_c)} \quad (8)$$

$$V_o = \frac{V_c \cdot K_o}{K_c \cdot S} \quad (9)$$

where  $V_c$  and  $V_o$  = maximum carboxylation and oxygenation velocities, respectively,  $K_c$  and  $K_o$  = carboxylation and oxygenation Michaelis constants, respectively,  $C_c$  and  $O_c$  = CO<sub>2</sub> and O<sub>2</sub> concentrations at Rubisco active sites, respectively, and  $S$  = Rubisco specificity for CO<sub>2</sub> relative to O<sub>2</sub>. Total resistance to CO<sub>2</sub> flux in the mutant,  $r_t$ , can be described as the sum of three resistances

$$r_t = r_g + r_{bs} + r_c \quad (10)$$

where  $r_g$  is gas phase resistance (boundary layer and stomatal),  $r_{bs}$  is liquid phase resistance (effectively BS resistance), and  $r_c$  describes carboxylation resistance of Rubisco. Gas phase resistance,  $r_g$ , was calculated from transpiration data. Intercellular CO<sub>2</sub> partial pressure,  $C_i$  equals

$$C_i = C_a - r_g A \quad (11)$$

where  $C_a$  is ambient CO<sub>2</sub> and  $A$  is net CO<sub>2</sub> assimilation rate. Intercellular CO<sub>2</sub> partitions between the gas phase and the cell wall liquid phase,  $C_w$  is

$$C_w = \beta_c C_i \quad (12)$$

giving soluble CO<sub>2</sub> where  $\beta_c$  is the CO<sub>2</sub> solubilization coefficient. The CO<sub>2</sub> concentration at the sites of carboxylation in the mutant,  $C_c$  is

$$C_c = C_w - r_{bs} A \quad (13)$$

O<sub>2</sub> concentration in the BS chloroplasts can be described as

$$O_c = O_m + a_w \cdot b \cdot r_{bs} \cdot A \quad (14)$$

where O<sub>2</sub> concentration at the mesophyll cell wall is

$$O_m = \beta_o O_i \quad (15)$$

$a_w$  is a constant that takes into account the difference in O<sub>2</sub> and CO<sub>2</sub> diffusivities (at 25°C  $a_w = 0.79$ ; Farquhar, 1983),  $b$  is the relative proportion of O<sub>2</sub> evolution in BS cells,  $O_i$  is the intercellular concentration of O<sub>2</sub>, and  $\beta_o$  is the O<sub>2</sub> partitioning factor between gaseous and liquid phase.

### DCDP Feeding Experiments

A leaf petiole was cut under water, and the CO<sub>2</sub> response curve was measured at 2% (v/v) oxygen (Fig. 3, A–C). Water was then replaced by a 4 mM solution of DCDP (PEPC inhibitor). After DCDP caused a decrease of photosynthesis to a stable level under atmospheric levels of CO<sub>2</sub> (about 20 min), the CO<sub>2</sub> response was measured (Fig. 3, B, D, and F). Measurement of photosynthesis on excised leaves can be problematic; however, using the FastEst gas exchange system the  $A/C_i$  response curves could be run in 20 min. The maximum rates of CO<sub>2</sub> fixation and response curves of control plants were similar to intact plants.

### Calculating BS Cell CO<sub>2</sub> Concentration and Leakiness in Wild-Type Plants

The mechanistic model of C<sub>4</sub> photosynthesis developed by von Caemmerer (2000) was used for estimating concentrations of CO<sub>2</sub> in BS cells. The model requires inputs for Rubisco kinetic parameters. The kinetic constants for *A. edulis* Rubisco ( $K_c = 16 \mu\text{M}$ ,  $K_o = 640 \mu\text{M}$ , and  $S = 82$  at 25°C) were obtained from the work of Jordan and Ogren (1983) and corrected for temperature according to Woodrow and Berry (1988).  $V_c$  was taken equal to the CO<sub>2</sub>-saturated assimilation rate at a PFD of 1,800  $\mu\text{mol m}^{-2} \text{s}^{-1}$ .

Leakiness of CO<sub>2</sub> from BS cells during photosynthesis in wild-type plants was calculated as a fraction of the rate of the C<sub>4</sub> cycle based on the above estimates of BS cell CO<sub>2</sub> concentration and measured values of  $r_{bs}$  in the *A. edulis* mutant, where the rate of leakage of CO<sub>2</sub> per unit leaf area ( $L_a$ ) equals

$$L_a = ([\text{CO}_2]_{\text{BS}} - [\text{CO}_2]_i) / r_{bs} \quad (16)$$

with  $[\text{CO}_2]_{\text{BS}}$  and  $[\text{CO}_2]_i$  representing the level of CO<sub>2</sub> in BS cells versus the external concentration in the intercellular air space, respectively. Leakiness ( $L$ ), from BS cells as a fraction of the rate of the C<sub>4</sub> cycle is defined as

$$L = L_a / (L_a + A) \quad (17)$$

### Measurement of RuBP Content

Leaf metabolism was stopped by quick filling of the leaf chamber with cooled ethanol (approximately –90°C). The frozen leaf (8 cm<sup>2</sup>) was then removed from the chamber and ground into a fine powder in a small mortar under liquid nitrogen. The powder was then transferred into 3 mL of 1 M HClO<sub>4</sub> and extracted for 15 min. The extract was neutralized with 5 M KOH and centrifuged 3 min at 5,000g. The supernatant was stored under liquid N<sub>2</sub> until analyzed. RuBP content was determined using the method of <sup>14</sup>C incorporation into acid stable product as in Prinsley et al. (1986) using purified Rubisco from tobacco (*Nicotiana tabacum*).

### Rubisco and Chlorophyll Content

For Rubisco activity measurements, the leaves were sampled the same way as for RuBP determination. The frozen leaf powder was then transferred into CO<sub>2</sub>-free 100 mM HEPES/KOH buffer (pH = 7.9). The Rubisco extraction buffer (1 mL per cm<sup>2</sup> of leaf) contained 20 mM MgCl<sub>2</sub>, 2 mM EDTA, and 5 mM dithiothreitol. It was then ground and homogenized in a Broeck Tissue Grinder (Corning, Palo Alto, CA) for about 20 s and divided into two parts, the first of which was immediately assayed by injecting 0.1 mL into a 0.9-mL assay medium and running the reaction 30 s at 28°C. This was taken as the in vivo activity of Rubisco. The assay media had the following final composition: 100 mM HEPES/KOH (pH = 7.9), 10 mM Mg<sup>2+</sup>, 2 mM EDTA, 5 mM dithiothreitol, 1 mM RuBP, and 10 mM NaHCO<sub>3</sub> + NaH<sup>14</sup>CO<sub>3</sub> with specific activity of 0.5 C<sub>i</sub> mol<sup>-1</sup>. The second assay, which was run after incubating the enzyme preparation 15 min in the presence of 10 mM NaHCO<sub>3</sub>, was taken as the fully carbamylated activity. It was shown, by adding purified Rubisco with known activities to leaf material before grinding, that there was no loss of activity attributable to extraction procedures. However, the possibility that some loss of activity may have occurred because of incomplete solubilization of Rubisco from the leaf material cannot be ruled out. The chlorophyll content of the leaves was determined according to Porra et al. (1989) using 80% (v/v) acetone extract.

### ACKNOWLEDGMENTS

We thank Dr. Colin Jenkins (Commonwealth Scientific and Industrial Research Organization, Canberra, Australia) for providing PEPC inhibitor DCDP. We appreciate discussion and some preliminary work with Dr. João Maroco (Instituto Superior de Agronomia, Lisbon, Portugal) on this project.

Received May 8, 2002; returned for revision June 16, 2002; accepted June 30, 2002.

### LITERATURE CITED

Brown RH (1997) Analysis of bundle sheath conductance and C<sub>4</sub> photosynthesis using a PEP-carboxylase inhibitor. *Aust J Plant Physiol* 24: 549–554

- Brown RH, Byrd GT** (1993) Estimation of bundle sheath cell conductance in  $C_4$  species and  $O_2$  insensitivity of photosynthesis. *Plant Physiol* **103**: 1183–1188
- Canvin DT, Berry JA, Badger MR, Fock H, Osmond CB** (1980) Oxygen exchange in leaves in the light. *Plant Physiol* **66**: 302–307 concentrating mechanism and photorespiration. *Plant Physiol* **103**: 83–90
- Dever LV, Blackwell RD, Fullwood NJ, Lacuesta M, Leegood RC, Onek LA, Pearson M, Lea PJ** (1995) The isolation and characterization of mutants of the  $C_4$  photosynthetic pathway. *J Exp Bot* **46**: 1363–1376
- Edwards GE, Baker NR** (1993) Can  $CO_2$  assimilation in maize leaves be predicted accurately from chlorophyll fluorescence analysis? *Photosynth Res* **37**: 89–102
- Edwards GE, Kiirats O, Laisk A, Okita TW** (2000) Requirements for the  $CO_2$  concentrating mechanism in  $C_4$  plants relative to limitations on carbon assimilation in rice. In JE Sheehy, PL Mitchell, B Hardy, eds, *Redesigning Photosynthesis in Rice*. International Rice Research Institute, Philippines, and Elsevier Science BV, Amsterdam, pp 99–112
- Ehleringer J, Bjorkman O** (1977) Quantum yields for  $CO_2$  uptake in  $C_3$  and  $C_4$  plants. *Plant Physiol* **59**: 86–90
- Evans JR, von Caemmerer S** (1996)  $CO_2$  diffusion inside leaves. *Plant Physiol* **110**: 339–346
- Evans JR, von Caemmerer S, Satchell BA, Hudson GS** (1994) The relationship between  $CO_2$  transfer conductance and leaf anatomy in transgenic tobacco with a reduced content of Rubisco. *Aust J Plant Physiol* **21**: 475–495
- Farquhar GD** (1983) On the nature of carbon isotope discrimination in  $C_4$  species. *Aust J Plant Physiol* **10**: 205–226
- Farquhar GD, von Caemmerer S, Berry JA** (1980) A biochemical model of photosynthetic  $CO_2$  assimilation in leaves of  $C_3$  species. *Planta* **149**: 78–90
- Furbank RT, Badger MR** (1982) Photosynthetic oxygen exchange in attached leaves of  $C_4$  monocotyledons. *Aust J Plant Physiol* **9**: 553–558
- Furbank RT, Jenkins CLD, Hatch MD** (1989)  $CO_2$  concentrating mechanism of  $C_4$  photosynthesis: permeability of isolated bundle sheath cells to inorganic carbon. *Plant Physiol* **91**: 1364–1371
- Genty B, Briantais J-M, Baker NR** (1989) The relationship between the quantum yield of photosynthetic electron transport and quenching of chlorophyll fluorescence. *Biochim Biophys Acta* **990**: 87–92
- Hatch MD, Agostino A, Jenkins CLD** (1995) Measurement of the leakage of  $CO_2$  from bundle-sheath cells of leaves during  $C_4$  photosynthesis. *Plant Physiol* **108**: 173–181
- He D, Edwards GE** (1996) Estimation of diffusive resistance of bundle sheath cells to  $CO_2$  from modeling of  $C_4$  photosynthesis. *Photosynth Res* **49**: 195–208
- Henderson SA, von Caemmerer S, Farquhar GD** (1992) Short-term measurements of carbon isotope discrimination in several  $C_4$  species. *Aust J Plant Physiol* **19**: 263–285
- Jenkins C, Furbank RT, Hatch M** (1989a) Inorganic carbon diffusion between  $C_4$  mesophyll and bundle sheath cells: direct bundle sheath  $CO_2$  assimilation in intact leaves in the presence of an inhibitor of the  $C_4$  pathway. *Plant Physiol* **91**: 1356–1363
- Jenkins C, Furbank RT, Hatch MD** (1989b) Mechanism of  $C_4$  photosynthesis: a model describing the inorganic carbon pool in bundle sheath cells. *Plant Physiol* **91**: 1372–1381
- Jordan DB, Ogren WL** (1983) Species variation in kinetic properties of ribulose 1,5-bisphosphate carboxylase/oxygenase. *Arch Biochem Biophys* **327**: 425–433
- Jordan DB, Ogren WL** (1984) The  $CO_2/O_2$  specificity of ribulose 1,5-bisphosphate carboxylase/oxygenase. *Planta* **161**: 308–313
- Kanai R, Edwards GE** (1999) Biochemistry of  $C_4$  photosynthesis. In RF Sage, RK Monson, eds, *The Biology of  $C_4$  Photosynthesis*. Academic Press, New York, pp 49–87
- Ku MB, Edwards GE** (1975) Photosynthesis in mesophyll protoplasts and bundle sheath cells of various types of  $C_4$  plants: IV. Enzymes of respiratory metabolism and energy utilizing enzymes of photosynthetic pathways. *Z Pflanzenphysiol* **77**: 16–32
- Labate CA, Adcock MD, Leegood RC** (1990) Effect of temperature on photosynthetic carbon assimilation and contents of photosynthetic intermediates in leaves of maize and barley. *Planta* **181**: 547–554
- Lacuesta M, Dever V, Munoz-Rueda A, Lea PJ** (1997) A study of photorespiratory ammonia production in the  $C_4$  plant *Amaranthus edulis*, using mutants with altered photosynthetic capacities. *Physiol Plant* **99**: 447–455
- Laisk A, Edwards GE** (1998) Oxygen and electron flow in  $C_4$  photosynthesis: Mehler reaction, photorespiration and  $CO_2$  concentration in the bundle sheath. *Planta* **205**: 632–645
- Laisk A, Edwards GE** (2000) A mathematical model of  $C_4$  photosynthesis: the mechanism of concentrating  $CO_2$  in NADP-malic enzyme type species. *Photosynth Res* **66**: 199–224
- Laisk A, Loreto F** (1996) Determining photosynthetic parameters from leaf  $CO_2$  exchange and chlorophyll fluorescence. *Plant Physiol* **110**: 903–912
- Laisk A, Oja V** (1998) Dynamics of Leaf Photosynthesis. Commonwealth Scientific and Industrial Research Organization Publishing, Collingwood, Australia
- Leegood RC, von Caemmerer S** (1988) The relationship between contents of photosynthetic metabolites and the rate of photosynthetic carbon assimilation in leaves of *Amaranthus edulis* L. *Planta* **174**: 253–262
- Maroco JP, Ku MSB, Furbank RT, Lea PJ, Leegood RC, Edwards GE** (1998a)  $CO_2$  and  $O_2$  dependence of PSII activity in  $C_4$  plants having genetically produced deficiencies in the  $C_3$  and  $C_4$  cycle. *Photosynth Res* **58**: 91–101
- Maroco JP, Ku MSB, Lea P, Leegood R, Furbank R, Edwards GE** (1998b) Oxygen requirement and inhibition of  $C_4$  photosynthesis: an analysis of  $C_4$  plants deficient in the  $C_3$  and  $C_4$  cycles. *Plant Physiol* **116**: 823–832
- Nobel PS** (1991) *Physicochemical and Environmental Plant Physiology*. Academic Press, New York
- Porra RJ, Thompson WA, Kriedemann PE** (1989) Determination of accurate extinction coefficients and simultaneous equations for assaying chlorophyll *a* and *b* with four different solvents: verifications of the concentrations of chlorophyll standards by atomic absorption spectroscopy. *Biochim Biophys Acta* **975**: 384–394
- Prinsley RT, Dietz K-J, Leegood RC** (1986) Regulation of photosynthetic carbon assimilation in spinach leaves after a decrease of irradiance. *Biochim Biophys Acta* **849**: 254–263
- Servaites JC, Geiger DR** (1995) Regulation of ribulose 1,5-bisphosphate carboxylase/oxygenase by metabolites. *J Exp Bot* **46**: 1277–1283
- von Caemmerer S** (2000) *Biochemical Models of Leaf Photosynthesis*. Commonwealth Scientific and Industrial Research Organization Publishing, Collingwood, Australia
- Woodrow IE, Berry JA** (1988) Enzymatic regulation of photosynthetic  $CO_2$  fixation in  $C_3$  plants. *Annu Rev Plant Physiol Plant Mol Biol* **39**: 533–594

# CORRECTIONS

Vol. 130: 964–976, 2002

Kiirats O., Lea P.J., Franceschi V.R., and Edwards G.E. Bundle sheath diffusive resistance to CO<sub>2</sub> and effectiveness of C<sub>4</sub> photosyntheses and refixation of photorepired CO<sub>2</sub> in a C<sub>4</sub> 0 cycle mutant and wild-type *Amaranthus edulis*.

The correct Figure 12 for the above article appears below.

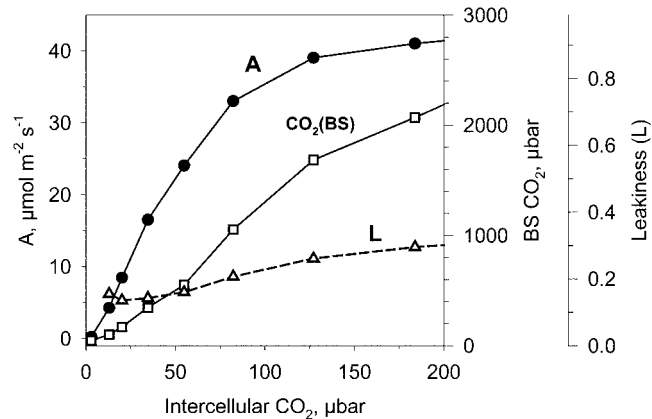


Figure 12. CO<sub>2</sub> response for CO<sub>2</sub> assimilation rate at leaf temperature of 28°C; PFD = 1,800 μmol m<sup>-2</sup> s<sup>-1</sup> (●), calculated CO<sub>2</sub> partial pressure in BS cells (◻), and leakiness of CO<sub>2</sub> from BS cells (Δ). The CO<sub>2</sub> level in BS cells was calculated according to von Caemmerer (2000), and the leakiness was calculated according to equations 16 and 17 using  $r_{bs}$  value of 113 m<sup>2</sup> s<sup>-1</sup> mol<sup>-1</sup>. Similar results were obtained from analysis of several experiments on A/Ci responses.

Vol. 131: 1250–1257, 2003

Pilon M., Owen J.D., Garifullina G.F., Kurihara T., Mihara H., Esaki N., and Pilon-Smits E.A.H. Enhanced Selenium Tolerance and Accumulation in Transgenic Arabidopsis Expressing a Mouse Selenocysteine Lyase.

The labeling of two bar graphs in Figure 5 of the above article is incorrect. The bar graph labeled 50 E' M SeCys should be labeled 50 E' M SeO4<sup>2-</sup>. The graph labeled 50 E' M SeO4<sup>2-</sup> should be labeled 50 E' M SeCys. The authors apologize for this error.

Vol. 131: 1781–1791, 2003

Tripathy S., Kleppinger-Sparace K., Dixon R.A., and Chapman K.D. N-Acylethanolamine Signaling in Tobacco Is Mediated by a Membrane-Associated, High-Affinity Binding Protein.

Dr. Kathryn F. Kleppinger Sparace was listed erroneously at the University of North Texas. Her current address is The Department of Genetics and Biochemistry, Clemson University, Clemson, SC 29634. The work was done at the University of North Texas, funded from a grant and salary provided by the Samuel R. Noble Foundation.